



Tree Physiology 00, 1–13
doi:10.1093/treephys/tpy083



Methods paper

Mitigating the open vessel artefact in centrifuge-based measurement of embolism resistance

Rosana López ^{1,2,5}, Markus Nolf³, Remko A. Duursma³, Eric Badel¹, Richard J. Flavel⁴, Hervé Cochard¹ and Brendan Choat³

¹Université Clermont Auvergne, INRA, PIAF, 5, chemin de Beaulieu, 63000 Clermont-Ferrand, France; ²Sistemas y Recursos Naturales, Universidad Politécnica de Madrid, C/ José Antonio Novais 10, 28040 Madrid, Spain; ³Hawkesbury Institute for the Environment, Western Sydney University, Hawkesbury Campus, Locked Bag 1797, 2751 Penrith, NSW, Australia; ⁴School of Environmental and Rural Science, University of New England, Elm Avenue, 2351 Armidale, NSW, Australia; ⁵Corresponding author (rosana.lopez@upm.es) 
orcid.org/0000-0003-3553-9148

Received May 4, 2018; accepted July 3, 2018; handling Editor Roberto Tognetti

Centrifuge-based techniques to assess xylem vulnerability to embolism are increasingly being used, although we are yet to reach a consensus on the nature and extent of artefactual embolism observed in some angiosperm species. In particular, there is disagreement over whether these artefacts influence both the spin (Cavitron) and static versions of the centrifuge technique equally. We tested two methods for inducing embolism: bench dehydration and centrifugation. We used three methods to measure the resulting loss of conductivity: gravimetric flow measured in bench-dehydrated and centrifuged samples (static centrifuge), in situ flow measured under tension during spinning in the centrifuge (Cavitron) and direct imaging using X-ray computed microtomography (microCT) observations in stems of two species of *Hakea* that differ in vessel length. Both centrifuge techniques were prone to artefactual embolism in samples with maximum vessel length longer than, or similar to, the centrifuge rotor diameter. Observations with microCT indicated that this artefactual embolism occurred in the outermost portions of samples. The artefact was largely eliminated if flow was measured in an excised central part of the segment in the static centrifuge or starting measurements with the Cavitron at pressures lower than the threshold of embolism formation in open vessels. The simulations of loss of conductivity in centrifuged samples with a new model, CAVITOPEN, confirmed that the impact of open vessels on the vulnerability to embolism curve was higher when vessels were long, samples short and when embolism is formed in open vessels at less negative pressures. This model also offers a robust and quantitative tool to test and correct for artefactual embolism at low xylem tensions.

Keywords: CAVITOPEN, Cavitron, centrifuge technique, drought, vulnerability to embolism, X-ray microCT, xylem embolism.

Introduction

Xylem water transport is dependent upon water held in a metastable state of water; evaporation of water from the leaf cell walls generates tension, which is transmitted through the water column to the roots. Water under tension is prone to cavitation, i.e., the abrupt transition from a metastable liquid to a gas, resulting in the formation of gas emboli that block the xylem conduits and impair water transport (Tyree and Sperry 1988). As tension in the xylem sap increases, for example during drought, so does the probability of embolism formation. During severe or

prolonged droughts, hydraulic failure can result in the complete loss of hydraulic conductance in the xylem and subsequent canopy dieback, or whole plant death (Brodribb and Cochard 2009, Nardini et al. 2013, Urli et al. 2013, Venturas et al. 2016, Rodríguez-Calcerrada et al. 2017). Hydraulic failure is now considered a principal cause of drought-induced plant mortality and forest die off (Sala et al. 2010, Choat et al. 2012, 2018). The projected rise in global mean temperature and frequency of extreme climate events over the next century will impact forest ecosystems and shift species distribution ranges. In this sense, resistance to embolism has emerged as a crucial parameter to

understanding species ecology, differences in water use strategies, and for predicting future mortality events (Brodrribb 2017).

Xylem resistance to embolism is usually characterized with a vulnerability curve (VC), showing the decrease in hydraulic conductivity as a function of the xylem tension. Since the publication of the first VCs for woody plants were published in 1985 (Sperry 1985) and 1986 (Tyree and Dixon 1986), a number of techniques that allow for more rapid measurement of vulnerability have been introduced (see Cochard et al. (2013) for a detailed review). However, although the time required for construction of a VC has been dramatically reduced, recent work suggests that some of these methods are prone to experimental artefact (Choat et al. 2010, Cochard et al. 2010, Sperry et al. 2012, Torres-Ruiz et al. 2014). This has led to re-examination of methodology used to measure vulnerability to embolism (Jansen et al. 2015).

The most straightforward technique for inducing embolism is bench dehydration, wherein whole plants or long branches are gradually dehydrated to various xylem tensions and hydraulic conductivity of excised segments is measured gravimetrically before and after removing air from embolized conduits (Sperry and Tyree 1988, Tyree and Zimmermann 2002). Bench dehydration relies on natural desiccation of plant tissues and is therefore considered as the best reference method with which to validate other techniques (Ennajeh et al. 2011, Sperry et al. 2012, Cochard et al. 2013). This method is not completely free of artefacts and issues associated with disequilibrium in water potential within a stem, blockage of flow by resin/mucilage (Cobb et al. 2007) and excision of samples under tension can all alter the VC significantly (Wheeler et al. 2013). Although most of these issues can be minimized by adoption of suitable protocols (e.g., Torres-Ruiz et al. 2015), the bench dehydration technique requires several days and a substantial amount of plant material to obtain a VC for one species. As such, Holbrook et al. (1995) and Pockman et al. (1995) proposed the use of a centrifugal force to create a defined negative pressure in the xylem sap of excised plant stems, allowing for rapid and consistent generation of VCs. Pockman et al. (1995) constructed VCs for several species by comparing the hydraulic conductivity before and after spinning branches with their ends exposed to air, removing segments at both ends before measuring conductivity in the remaining, middle section of the sample. Alder et al. (1997) modified this technique with a centrifuge rotor designed to keep the segment ends immersed in water during spinning, allowing the conductivity of a single segment to be remeasured at different tensions to create an entire VC for a single sample. This important innovation allowed repeated measurements to be made on the same plant material, reducing the number of samples required for construction of a curve and strengthening the results statistically. Finally, Cochard (2002), Cochard et al. (2005) and Li et al. (2008) further modified the centrifuge method and designed

new rotors which allowed measurement of conductivity of the segment while it is spinning and under tension. This further increased the efficiency of measurement and allowed for flow measurements to be made under tension.

Although centrifuge-based techniques induce embolism by increasing tension in sample xylem, the patterns of embolism spread through the sample may differ from a naturally dehydrated sample (Cai et al. 2010). The tension profile in the centrifuged segment is highest in the axis of rotation (i.e., in the middle section of the segment) and declines towards the segment ends (Cochard et al. 2005), while during natural dehydration the tension profile across the segment is expected to remain approximately constant (Cai et al. 2010). Nevertheless, the VCs generated by centrifugation agree well with the benchmark method in conifers and short-vesselled angiosperm species (Alder et al. 1997, Cochard et al. 2005, 2010, Li et al. 2008). In contrast, inconsistent results have been obtained for species with long vessels, specifically those in which a significant number of vessels in the sample are longer than the centrifuge rotor (Choat et al. 2010, Jacobsen and Pratt 2012, Sperry et al. 2012, Torres-Ruiz et al. 2014).

Since 2005 the number of VCs constructed by centrifugation has increased exponentially (see Figure 3 in Cochard et al. (2013)). Accordingly, considerable effort has been devoted to testing and validation of centrifuge techniques, whether measuring the flow gravimetrically after spinning (static centrifuge method) or while centrifuging (Cavitron method). However, we are yet to reach a consensus on the nature and extent of artefactual embolism observed with centrifuge techniques. In particular, there is disagreement over whether these artefacts influence both spin (Cavitron rotor) and static versions of the centrifuge technique equally (Sperry et al. 2012, Hacke et al. 2015). In recent years, the application of X-ray computed microtomography (microCT) to the study of plant hydraulics has emerged as a potentially powerful tool to validate hydraulic techniques. In addition to providing a non-invasive assay of xylem function, it allows for analyses of spatial and temporal patterns of embolism formation (Brodersen et al. 2013, Dalla-Salda et al. 2014, Choat et al. 2016, Torres-Ruiz et al. 2016).

In this study, we evaluated the performance of both centrifuge techniques against bench dehydration in order to examine possible discrepancies associated with each technique. First, we tested two methods for inducing embolism: bench dehydration and centrifugation. We then tested three ways of measuring the resulting loss of conductivity: gravimetric flow measured in bench-dehydrated and centrifuged samples (static centrifuge), in situ flow measured under tension during spinning in the centrifuge (Cavitron) and direct imaging using X-ray microCT observation. All experiments were carried out with two species of the genus *Hakea* that differ in vessel length. *Hakea dactyloides* is a short-vesselled species with maximum vessel length shorter than 14 cm, whereas *Hakea leucoptera* has longer vessels and

maximum vessel length is ~25 cm. Additionally, we compared results obtained using two rotor diameters (14 and 27 cm) to assess the effect of sample length, and measured hydraulic flow both in the whole, spun segments and excised middle sections. Spatial patterns of embolism within samples were visualized with X-ray microCT after centrifugation in order to provide further insight into potential discrepancies. Finally, a new model, CAVITOPEN, was developed to simulate the effect of vessel and sample lengths on centrifuge estimates of embolism resistance. We hypothesized that (i) both centrifuge techniques, the static centrifuge and the Cavitron, are prone to similar artefacts when constructing VCs of long-vessel species; (ii) the shape of the VC of centrifuged samples will depend on the amount of cut open vessels; and (iii) image techniques and standard flow measurements will produce similar VCs.

Materials and methods

Plant material

Experiments were carried out on branch material of two diffuse-porous species of the same genus exhibiting different vessel lengths, *Hakea dactyloides* (Gaertn.) Cav. and *Hakea leucoptera* R. Br. Branches were sampled from natural populations of *H. dactyloides* at Mount Banks (33° 34' 46' S, 150° 21' 56' E; NSW, Australia) and *H. leucoptera* at Binya State Forest (34° 11' 16' S, 146° 16' 13' E; NSW, Australia) from May to September 2016 (late autumn-winter in the southern hemisphere). Sun-exposed branches of 1.5–2.0 m length were collected in the field in the early morning and immediately placed in black plastic bags with moistened paper towels to prevent transpiration with their cut ends covered with Parafilm. In the laboratory they were kept at 4 °C until measured.

Midday xylem water potential in the field and native embolism

Midday xylem water potential was measured in the field in November 2015, February 2016 and June 2016. Two leaves of five plants per species were covered with aluminium foil and sealed with a plastic bag 1 h before excision and measurement with a pressure chamber (PMS Instrument Co., Albany, OR, USA).

Native embolism was determined in current-year, 1-year-old and 2-year old segments of five branches per species to ensure that the effects of previous natural water stress were minimized. Note that segments containing 1 and 2-year-old growth were necessary to fit in the 27 cm rotor of the centrifuge. Measuring native embolism we also wanted to control for sample collection date because branches were cut at different times during late autumn-winter 2016 to avoid long storage. Branch proximal end was cut under water to release tension for 30 min (Wheeler et al. 2013, Torres-Ruiz et al. 2015) and then the branch was progressively recut under water to segments 50 mm long. Note

that at least twice the maximum vessel length was removed from the cut end after tension relaxation. Thereafter, the edges of these segments were trimmed using a razor blade. Initial conductivity (K_h) was measured in 50 mm long segments with filtered, degassed 2 mmol KCl solution at low pressure (≤ 4 kPa) with a liquid flowmeter (LiquiFlow L13-AAD-11-K-10S; Bronkhorst High-Tech B.V., Ruurlo, The Netherlands). The segments were then flushed with the same solution at a minimum of 0.20 MPa for 15 min to remove embolism and subsequently determine maximum hydraulic conductivity (K_{max}). The native percentage loss of conductivity (PLC) was calculated for each segment as:

$$PLC = 100 \times (1 - K_h/K_{max}) \quad (1)$$

Specific hydraulic conductivity (K_S) was calculated dividing K_{max} by the xylem cross-sectional area (average distal and proximal xylem area measured with a calliper).

Maximum vessel length and vessel length distribution

Ten branches per species were sampled from the same plants as used for hydraulic measurements to determine maximum vessel length with the air perfusion technique (Ewers and Fisher 1989). Once in the lab, 60 cm long segments were flushed for 1 h with degassed, filtered 2 mmol KCl solution at 0.18–0.20 MPa to remove any embolism. Then each segment was infiltrated with compressed air at 0.05 MPa at its distal end with an aquarium air pump while the basal end was repeatedly shortened by 2 cm under water until air bubbles emerged. The remaining sample length was assumed as maximum vessel length.

An estimate of the amount of vessels longer than the centrifuge rotor diameter and longer than half the rotor diameter (open to centre vessels) was assessed in four branches of *H. dactyloides* and five branches of *H. leucoptera* by measuring the decrease in PLC after air injection (Cochard et al. 1994, Torres-Ruiz et al. 2014). Briefly, 35 cm long segments were flushed as described above to remove embolism. Then, tubing was attached to the distal end of these segments and compressed air was injected into the samples at 0.1 MPa for 10 min using a pressure chamber. This pressure was sufficient to empty the open vessels but not high enough to move water through wet pit membranes between adjacent vessels (Ewers and Fisher 1989). Percentage loss of conductivity was determined in 3 cm long segments across the sample as described for native embolism. At the injection point, PLC is close to 100% because all the vessels are air filled and progressively decrease to 0 for a length longer than the longest vessel in the sample. The PLC at each distance from the injection point corresponds to the percentage of contribution to flow from vessels longer than this distance. If all the vessels were of equal diameter, this percentage would correspond to the number of vessels longer than the distance from the injection point. In this case the two *Hakea* species used are diffuse porous and vessel diameters within the same sample

did not vary greatly. Thus the curves in Figure 1 represent a proxy of vessel distribution of the two species, although not as accurate as anatomy, and allow to estimate the amount of open vessels from a certain cut point.

Bench dehydration technique

Branches were dehydrated gradually in the laboratory at $\sim 23^\circ\text{C}$. Xylem water potential (Ψ_x) was measured with a pressure chamber (PMS Instrument Co.) in bagged leaves (wrapped with aluminium foil and a plastic bag at least 1 h before sampling). When the target Ψ_x to construct the VC was reached, branches were sealed into a plastic bag with moistened paper towels for 1 h to equilibrate Ψ_x . Water potential was measured again in two bagged leaves of the same branchlet to confirm homogeneous Ψ_x in the sample. The Ψ_x of the sample was considered equilibrated if the difference between the three Ψ_x (one measured before sealing the branch and two measured after equilibration) was not higher than 0.1 MPa. Afterwards tension was released for 30 min by cutting the branch proximal end under water and PLC was determined in 1-year-old segments as for native embolism. Vulnerability curves were generated by plotting PLC against Ψ_x . For *H. leucoptera* seven branches were dehydrated and four different branchlets per branch were measured at different Ψ_x to construct the VC and for *H. dactyloides* we used 12 branches and two branchlets per branch. All branchlets were far apart (at least four branch orders) and after collection the cutting surface was covered with parafilm to avoid air entry in the rest of the sample.

Centrifuge techniques

We compared two centrifuge techniques: (i) the static centrifuge method described by Alder et al. (1997) and (ii) the in situ flow centrifuge technique (Cavitron (Cochard 2002, Cochard et al. 2005)). In the static centrifuge two different sizes of custom-built rotors,

14 cm and 27 cm, were used to test the effect of segment length and fraction of open vessels. All hydraulic conductivity measurements were performed using filtered, degassed 2 mmol KCl solution and a flow metre (see Minimum xylem water potential and native embolism in the field).

Static centrifuge measurements were carried out on 20 branches per species. Branches were trimmed under water and both ends were shaved to a final length of 14 or 27 cm. The initial hydraulic conductivity was measured as described above (see Midday xylem water potential in the field and native embolism section) with a pressure head of 7.5 kPa. Subsequently, 14-cm long branches were spun in the centrifuge (Sorvall RC 5 C Plus) for 5 min at increasing pressure steps. Foam pads saturated with the solution used for measurements were placed in the reservoirs of the rotor to maintain sample ends in contact with the solution even when the rotor was stopped (Tobin et al. 2013). After each step, samples were removed and K_h was measured on the whole segment as described for native embolism. In the 27 cm long branches we modified the single spin method (Hacke et al. 2015) so that two measurements were made in each centrifuged segment. The initial K_h was measured before spinning in the 27 cm long sample. After spinning, K_h was measured on the whole segment and the first PLC was calculated. Subsequently, a 4 cm long segment was cut from the middle section and its K_h was measured. The second PLC was determined in this 4 cm long segment after flushing to obtain the maximum K_h (K_{max}) as described for native embolism.

In situ flow centrifuge measurements (Cavitron technique) were carried out on six branches per species using a modified bench top centrifuge (H2100R, Cence Xiangyi, Hunan, China). For the static centrifuge, samples were trimmed under water to a length of 27 cm to fit in the rotor. Initial conductivity, K_i , was determined at a xylem pressure of -0.5 MPa in *H. dactyloides* and 1.5 MPa in *H. leucoptera*. The xylem pressure was then lowered stepwise by increasing the rotational velocity, and K_h was again determined while the sample was spinning. The PLC at each pressure step was quantified as

$$\text{PLC} = 100 \cdot (1 - K_h/K_i) \quad (2)$$

X-ray microCT imaging

A subset of branches of *H. leucoptera* was transported to the University of New England in Armidale (NSW, Australia). They were gradually dehydrated to five different xylem water potentials ranging from -4.8 to -9 MPa as for the bench dehydration method. After measuring Ψ_x , tension was relaxed by cutting the proximal end of the branch under water leaving it submerged for 30 min. Then the branch was sequentially cut back under water and finally 10 mm long segments were excised under water from current-year shoots, wrapped in Parafilm, inserted into a plexiglass tube and then placed in an X-ray microCT system (GE-Phoenix Vtomeixs, GE Sensing & Inspection Technologies, Wunstorf, Germany) to visualize embolized

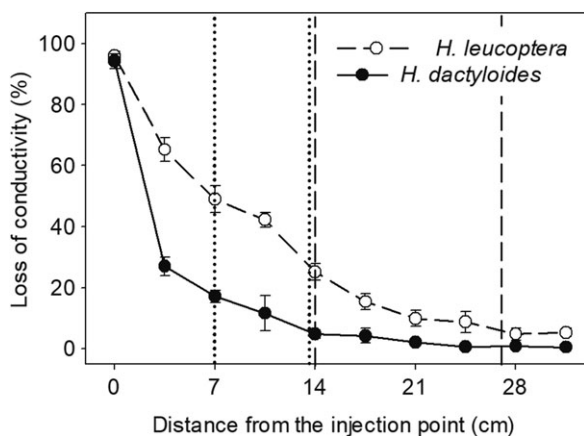


Figure 1. Distribution of PLC in air-injected branches of *H. dactyloides* (black circles) and *H. leucoptera* (open circles) at different positions from the injected end. Vertical bars represent the standard error. Dashed lines indicate the two sample lengths used for the centrifuge methods, 14 cm and 27 cm and dot lines indicate their respective half sample length.

vessels. Another subset of branches of *H. leucoptera* was centrifuged to five (−5, −6, −7, −8, −9 MPa) and three (−5, −6, −7 MPa) different water potentials in the static centrifuge using 27 cm and 14 cm long segments, respectively. They were immediately submerged in liquid paraffin wax and preserved at 4 °C for 3 days until measured in the same facility (Cochard et al. 2015). Seven branches of *H. dactyloides* were also centrifuged at four (−3, −4, −5, −6 MPa) and three (−3, −4, −5 MPa) water potentials with the 27 and 14 cm rotors, respectively, following the same protocol. One branch of *H. leucoptera* was prepared as the centrifuged samples but was not spun in the centrifuge to detect any possible artefact due to sample preparation. All samples were scanned at the middle of the sample. Additionally, in three 27 cm long samples we scanned at 6 cm and 12 cm from the axis of rotation to examine embolism profiles across a sample.

X-ray scan settings were 90 kV and 170 mA, and 1800 projections, 600 ms each, were acquired during the 360° rotation of the sample. The resultant images covered the whole cross-section of the sample in 8.7 mm length with a spatial resolution of 8.7 µm per voxel. At the end of the scan, the sample was cut back to 30 mm length, injected with air at >1 MPa pressure and rescanned at the same location as before to visualize all empty vessels in the fully embolized cross-section. After three-dimensional reconstruction with Phoenix datosl x 2 Reconstruction Version 2.2.1-RTM (GE Sensing & Inspection Technologies), volumes were imported into ImageJ 1.49k (Schneider et al. 2012). A median Z projection of ~100 µm along the sample axis was extracted from the middle of the scan volumes following the protocol in Nolf et al. (2017). Percentage loss of conductivity of each sample was estimated calculating the theoretical hydraulic conductance based on the conduit dimensions of embolized and functional vessels (Choat et al. 2016). To measure conduit dimensions, a radial sector of the transverse section was selected in the same microCT scan and all their embolized vessels were measured manually. The image of this sector was then binarized so the dimensions of the selected embolized vessels matched with the manually drawn vessels. This threshold value was then used for binarizing the image of the whole cross-section and all the embolized vessels were measured using the Analyse Particles function in ImageJ. Theoretical specific hydraulic conductivity (K_{sth}) was calculated as:

$$K_{sth} = \frac{\sum \left(\frac{D^4 \pi}{128 \eta} \cdot \frac{\Delta p}{\Delta x} \right)}{A} \quad (3)$$

where D is the equivalent circular vessel diameter based on vessel area, η viscosity of water, $\Delta p/\Delta x$ pressure gradient per xylem length and A xylem cross-sectional area.

The current theoretical specific hydraulic conductivity (K_{sth}) for each sample was calculated by subtracting the summed specific hydraulic conductivity of embolized vessels from the $K_{sth(max)}$ of that sample, calculated as the K_{sth} of the sample after air injection. The pressure gradient used for calculations of K_{sth} was

similar to the pressure gradient used in the hydraulic measurements, 0.06 MPa m^{−1}.

Vulnerability curve fitting and statistical analysis

Vulnerability curves were fitted using a Weibull function (Ogle et al. 2009) in R 3.2.0 (R Development Core Team, 2015) using the fitplc package (Duursma and Choat 2017). Confidence intervals of P_{12} , P_{50} and P_{88} (Ψ_x at 12%, 50% and 88% loss of conductivity, respectively) and the slope of the curve at 50% loss of conductivity (S_{50}) were used to compare between methods. Confidence intervals (CIs) for the bench dehydration and the static centrifuge techniques were obtained using bootstrap resampling (999 replicates). Methods were considered to be statistically different if the 95% CIs did not overlap.

Differences in native embolism and specific initial conductivity between sampling dates were tested with a one-way ANOVA. Means were compared using a Tukey test at 95% confidence. Vulnerability curve parameters across methods were compared at the Ψ_x corresponding with three levels of loss of conductivity: 12%, 50% and 88% (P_{12} , P_{50} and P_{88} , respectively) and the slope of the VC at 50% loss of conductivity (S_{50}).

CAVITOPEN-simulation of the effect of open vessels in a centrifuged sample

To disentangle the effects of centrifugation on 'true' vessel embolism at the centre of the samples, where more vessels are closed at both ends and tension is maximum, from draining of open vessels at both sample ends a new model, CAVITOPEN, was developed. In a centrifuged sample, the variation of xylem pressure (P) with distance from the axis of rotation (r) is given by the following equation (Alder et al. 1997):

$$dP/dr = \rho \omega^2 r \quad (4)$$

where ρ is the density of water and ω the angular velocity.

Integrating this equation from R (distance from the axis of rotation to the water reservoir) we can obtain the pressure at $r(P_r)$:

$$P_r = 0.5 \rho \omega^2 (R^2 - r^2) \quad (5)$$

The effect of vessel length on 'true' vessel embolism in a spun sample has already been modelled by Cochard et al. (2005). Briefly, if the vessels are infinitely long, the VC obtained by centrifugation should yield the correct P_{50} value. When the vessels are infinitely short the P_{50} value is underestimated due to the variation of xylem pressure inside the spun sample (Eq. (4)) and the consequent gradient of embolism along the sample: xylem pressure is minimum in the middle of the sample and null at the extremities (Eq. (5)). Since the loss of conductivity is measured on the whole sample, an underestimation of the degree of embolism in the middle of the sample is predicted. This effect of vessel length was further tested with the CAVITOPEN model and

found marginal, i.e., the shift in the VC was negligible, compared with the draining effect. For the sake of simplicity, this effect was no longer considered in the simulations. To simulate the draining effect at both sample ends, we first hypothesized that vessel ends follow a logarithmic distribution following the vessel length probability density function proposed by Cohen et al. (2003) and assuming vessel ends uniformly distributed across the length of the sample:

$$N_x = N_0 \cdot \exp(-x/L_{\max}) \quad (6)$$

where N_x is the number of open vessels at the distance x from sample ends, N_0 the total number of vessels and L_{\max} the maximum vessel length.

The second assumption of the model is that open vessels drain when the minimum pressure in the vessel exceeds a threshold value P_{open} . Because of the quadratic distribution of the pressure in the sample, vessels having their end wall located closer to the sample ends, i.e., further from the centre of rotation, will drain at a higher rotational velocity.

The branch segment was discretized in 0.1 mm thick sections arranged in serial. The xylem pressure in the middle of the segment was set to a pressure varying from 0 to -12 MPa in 1 MPa steps. The model then computes the pressure at steady state in each 0.1 mm section and determines the PLC caused by 'true' embolism (non-open vessels) and by draining (open vessels). Finally, the PLC of the whole segment is computed which enables the construction of the VC. We tested the model for different theoretical L_{\max} values and the four rotors sizes used in our experiments. To validate the model we used the values of PLC obtained for *H. leucoptera* in the static centrifuge with the 27 cm rotor. The CAVITOPEN model was fit to the measurements using constrained numerical optimization to estimate four parameters: P_{50} , S_{50} , L_{\max} and P_{open} . All routines were implemented as an R package (available from Duursma 2017).

Results

Native embolism and minimum xylem water potential in the field

Midday xylem water potential decreased from -1.02 to -1.51 MPa in *H. dactyloides* and from -1.35 to -2.62 MPa in *H. leucoptera* from November 2015 to February 2016. In June 2016, the water potential was -1.16 MPa in *H. dactyloides* and -1.42 MPa in *H. leucoptera*. Native embolism remained low in both species across the sampling dates. We measured higher PLC in 2-year-old branch segments ($<13\%$) than in current-year growth ($<2\%$) in *H. leucoptera* whereas in *H. dactyloides* native embolism was lower than 2% in all samples. Maximum xylem specific conductivity (K_{smax}) was $0.87 \pm 0.10 \text{ kg m}^{-1} \text{ s}^{-1} \text{ MPa}^{-1}$ in *H. leucoptera* and $1.29 \pm 0.09 \text{ kg m}^{-1} \text{ s}^{-1} \text{ MPa}^{-1}$ in *H. dactyloides* (mean \pm SD). No significant differences in native

PLC or K_s ($P > 0.05$; see Table S1 available as Supplementary Data at *Tree Physiology* Online) were detected between sampling dates.

Maximum vessel length and vessel length distribution

Maximum vessel length as determined by air injection was 25 cm (SD = 5) in *H. leucoptera* and 10 cm (SD = 3) in *H. dactyloides*. Air-injected branches of *H. dactyloides* showed 17% PLC at 7 cm from the injection point, 5% at 14 cm and less than 1% at 28 cm, whereas in *H. leucoptera* the PLC was always higher, 50%, 25% and 5% at 7, 14 and 28 cm, respectively (Figure 1). Thus the number of open vessels at both ends when using the centrifuge technique differed between species.

Vulnerability curves

Vulnerability curves obtained with the bench dehydration technique were s-shaped for both species, with significant embolism only occurring once a threshold water potential had been reached. This threshold was more negative in *H. leucoptera* (-6.3 MPa) than in *H. dactyloides* (-3.8 MPa) (Figure 2). Vulnerability curves obtained with bench dehydration had the most negative P_{12} and the steepest slopes of all methods (see Table S2 available as Supplementary Data at *Tree Physiology* Online), meaning that embolism formation started at more negative Ψ_x and conductivity was lost across a narrower range of Ψ_x compared with VCs generated by centrifugation.

When the centrifuge was used to induce embolism, results in the shorter-vesseled species, *H. dactyloides*, were similar for the three techniques used to measure loss of conductivity, flowmeter, Cavitron and microCT (average P_{50} with the 27 cm rotor in the static centrifuge and the Cavitron -4.8 MPa), and the CI at 95% overlapped with bench dehydration ($P_{50} = -5.0$ MPa). The VC generated with the 14 cm rotor for *H. dactyloides* yielded slightly less negative values ($P_{50} = -4.3$ MPa; Figure 2; see Table S2 available as Supplementary Data at *Tree Physiology* Online). In contrast, VCs for *H. leucoptera* differed considerably depending on the method and the sample length. Vulnerability parameters (P_{12} , P_{50} , P_{88}) obtained with the Cavitron (-5.0 , -7.1 and -9.0 MPa, respectively) matched more closely with the bench dehydration VC (-6.3 , -7.4 and -8.2 MPa). For samples spun in the static centrifuge, we found a significant effect both of the rotor size and the segment used to measure flow (whole, spun segment or excised middle section in the 27 cm rotor) on apparent vulnerability to embolism: segments measured across their entire length exhibited higher vulnerability to embolism compared with the bench-dehydration VC as shown by P_{12} (-1.2 and -2.6 MPa for 14 and 27 cm rotors, respectively) and P_{50} (-5.3 and -6.0 MPa, respectively), but seemed less vulnerable towards the dry end of the curve (P_{88} of -14.2 and -10.4 MPa, respectively; see Table S2 available as Supplementary Data at *Tree Physiology* Online). Both VCs were almost linear when flow was measured across the whole

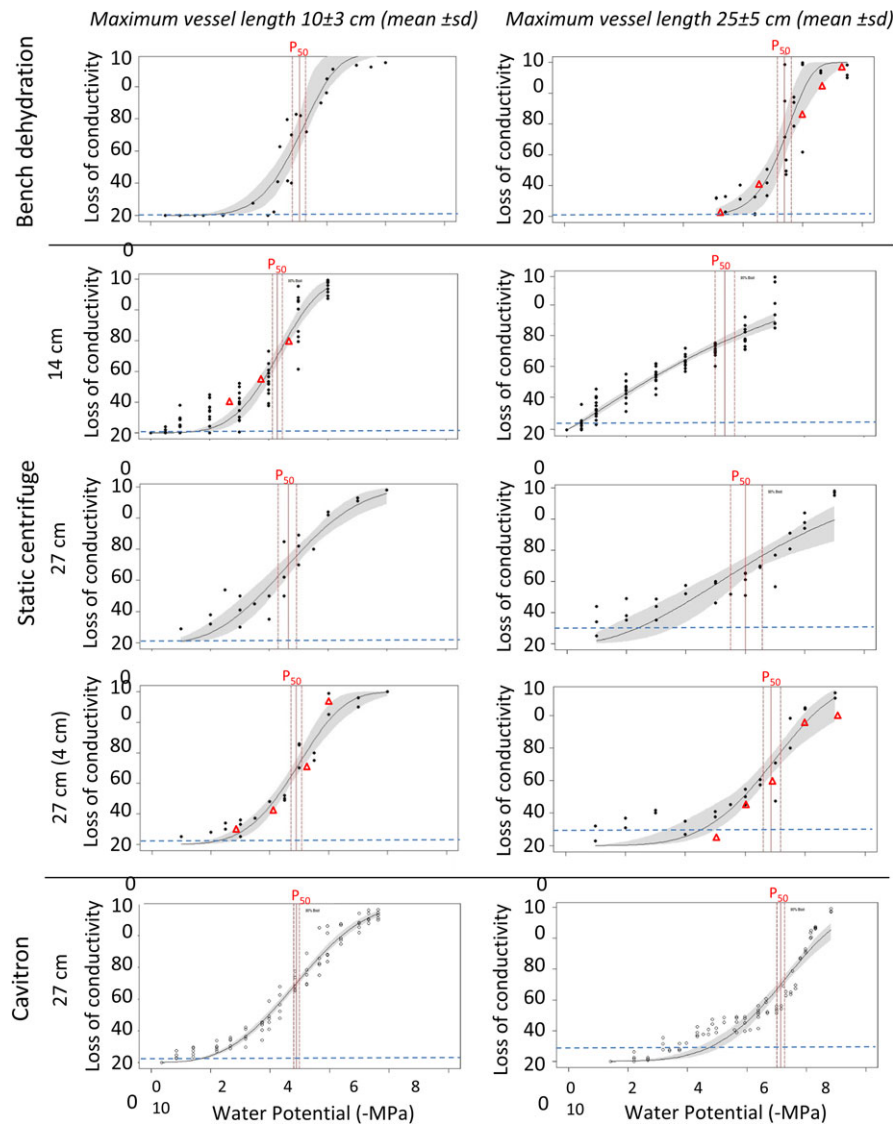


Figure 2. Xylem vulnerability to embolism curves and 95% CIs (grey shaded areas) of *H. dactyloides* (left panels) and *H. leucoptera* (right panels) obtained with two methods to induce cavitation in the xylem, bench dehydration and centrifuge force and three methods to measure the loss of conductivity, flowmeter (closed circles), in situ flow method (open circles) and X-ray microCT visualization (red triangles). Vertical solid lines indicate P_{50} and vertical dashed lines indicate the 95% CI for P_{50} . Horizontal dashed lines indicated native xylem embolism measured in the field. Two rotor sizes, 14 cm and 27 cm, were used in the static centrifuge, and water flow in the whole segment or only in the central part was measured (see Materials and methods for details).

segment with a shift towards more vulnerable values with the 14 cm rotor, but became s-shaped when only the middle section of the 27 cm segment was measured (Figure 2). Removing the segment ends resulted in a steeper slope and significantly more negative values of P_{12} and P_{50} . The Cavitron and the middle segment techniques yielded similar results and agreed well with the dehydration technique in P_{50} and P_{88} and with microCT image analysis (red triangles in Figure 2).

Patterns of embolism across a centrifuged sample

Within 27-cm-length centrifuged samples of *H. leucoptera*, microCT scans revealed that embolism levels were consistently at their

highest near the sample ends (at 12 cm from the axis of rotation) when spun at equivalents of -5 , -7 and -9 MPa in the static centrifuge (Figure 3). At -5 and -7 MPa loss of conductivity decreased from the basal end to the centre, contradicting theoretical expectations. This trend was observed even at Ψ_x inducing less than 40% PLC based on the bench dehydration VC (Figure 3). Only at -9 MPa, that is, below P_{88} on bench dehydration, did levels of embolism converge along the length of the sample at 80–90%.

Influence of open vessels in the VC of a centrifuged sample

The simulations produced by the CAVITOPEN model confirmed that the shape of the VCs generated by the centrifugation was

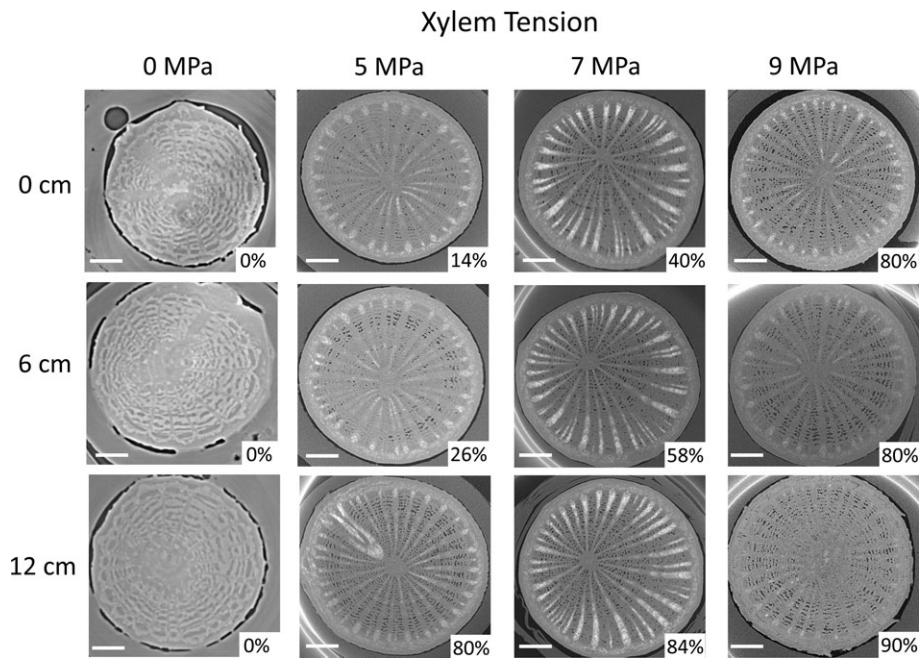


Figure 3. Transverse slices from X-ray micro-CT scans of branches of *H. leucoptera* (maximum vessel length = 25 ± 5 cm) scanned at three positions before spinning (left column) and after spinning in the centrifuge at 5, 7 and 9 MPa. Embolized vessels appear as black and water-filled conduits appear as grey. The estimated PLC is shown in each picture. Scale bar, 1 mm.

largely dependent on vessel and sample lengths. As maximum vessel length decreased, PLC of the whole sample decreased at a given Ψ_x , and the shape of the VC shifted from exponential to sigmoidal (Figure 4A). The same pattern was observed when the sample length increased (Figure 4B). For instance, with 14 cm length centrifuged samples, P_{50} ranged from -0.6 MPa to -7.7 MPa varying the maximum vessel length of the sample from 50 cm to 5 cm. Likewise, the P_{50} of a centrifuged sample with maximum vessel length of 15 cm ranged from -2.1 MPa in the 14-cm rotor to -7.7 MPa using a 40-cm rotor. Embolism of vessels open from the cut surface (see Figure S1 available as Supplementary Data at *Tree Physiology* Online) influenced values of PLC at high negative pressures, even in short-vesseled samples, resulting in rapid loss of conductivity followed by a plateau. The more open vessels and the less negative the threshold of embolism of open vessels (Figure 4C), the higher is this plateau and stronger the impact on the VC (Figure 4). Vulnerability curves can be corrected if the first inflection point of the curve is considered the starting point for initial conductivity (K_i), i.e., 0% loss of conductivity. This is shown in Figure 4D with actual measurements of PLC obtained in 27-cm centrifuged samples of *H. leucoptera*. When the CAVITOPEN model was fit (black circles and grey solid line, respectively) and we used the inflection point as starting point for K_i , the corrected curve matched the reference VC obtained with bench dehydration (Figure 4D black solid line and orange dashed line, respectively). Alternatively, by fitting the model using numerical optimization we estimated values of $P_{50} = -6.9$ MPa, $S_{50} = 49.7$, $L_{max} = 15.21$ and $P_{open} = -0.75$.

Discussion

We evaluated the reliability of two centrifuge-based techniques commonly used to measure vulnerability to embolism in angiosperm species and present a protocol that mitigates experimental artefacts associated with open xylem vessels. Both the static centrifuge method and the in situ flow centrifuge method (Cavitron) were prone to artefactual embolism caused by open vessels, although the errors were significantly greater in the static centrifuge method. In a species with maximum vessel length longer than or similar to the centrifuge rotor diameter, the static centrifuge significantly overestimated xylem vulnerability to embolism if the whole spun segment was used to measure flow. Observations with microCT indicated that artefactual embolism caused by centrifugation of samples occurred in the outermost portions of samples. However, we demonstrated that artefactual embolism was largely eliminated from static centrifuge if flow was measured in an excised central part of the segment. This altered protocol yielded VCs similar to those obtained on the same species with bench dehydration thus allowing these centrifuge techniques to accurately measure vulnerability to embolism in longer vesseled species. We also present a new model (CAVITOPEN) that simulates the impact of vessel draining at the cut end on the whole VC curve and showed that errors were largely dependent on vessel length and rotor diameter. This model allows researchers to quantitatively test and avoid errors associated with the artefactual embolism. The bench dehydration technique indicated that significant embolism was only initiated in both species after water potential dropped below a threshold

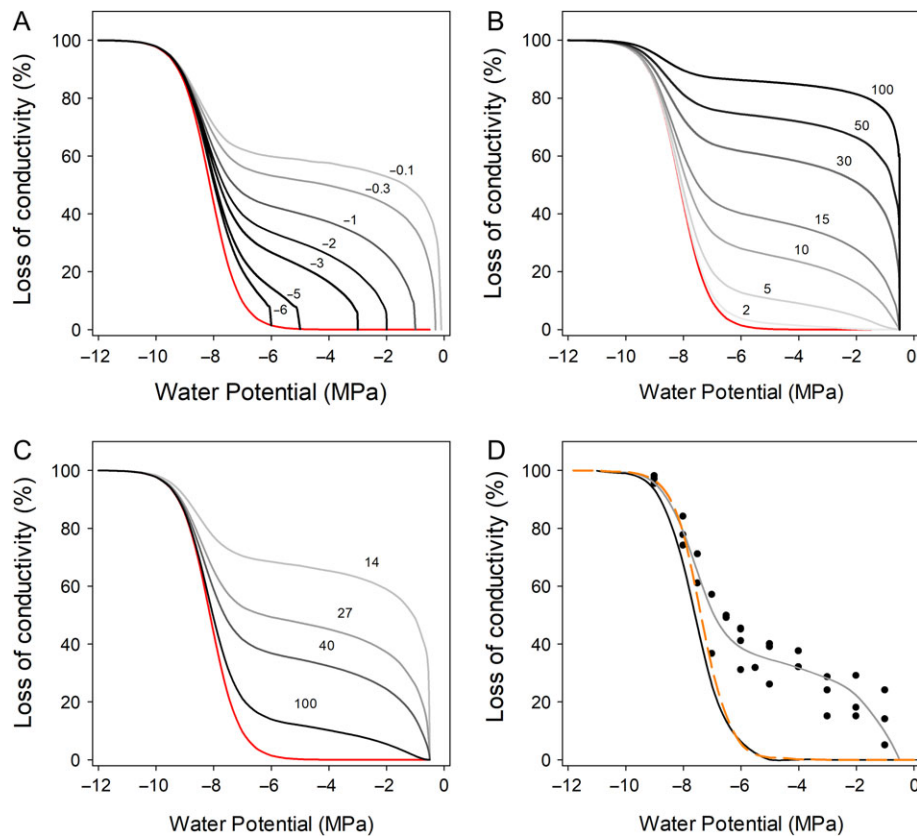


Figure 4. Simulations with the CAVITOPEN model of the effect of threshold of embolism formation (MPa) of cut open vessels (A), maximum vessel length (cm) (B) and rotor size (cm) (C) on xylem vulnerability to embolism curves generated with centrifugation. In red, VC of close vessels at both ends. (D) The CAVITOPEN model was fit to measurements in *H. leucoptera* using numerical optimization to estimate all four parameters: water potential at 50% loss of conductivity (P_{50}), slope of the VC (S_{50}), maximum vessel length (L_{max}) and threshold of embolism formation of cut open vessels (P_{open}). Circles represent the values obtained in our study with the static centrifuge, 27 cm rotor in *H. leucoptera* when flow was measured in the whole segment (see Materials and methods for details); grey solid line is the fitted curve with the CAVITOPEN model; black solid line represents the curve after correction and orange dashed line is the reference curve obtained with bench dehydration for the species.

value, -3.8 MPa in *H. dactyloides* and -6.3 MPa in *H. leucoptera*. Percentage loss of conductivity then increased rapidly and hydraulic conductivity was lost almost completely within a span of 1 MPa (Figure 2). These VCs have been classified as sigmoidal or s-shaped as opposed to exponential or r-shaped curves, characterized by rapid conductivity losses as soon as the water potential declines below zero (Sperry et al. 2012, Cochard et al. 2013). A third type of VC, intermediate between these two, exhibits a linear response, and is mainly found in diffuse porous species when using centrifugation to induce embolism (Cochard et al. 2013).

Our results showed that VCs obtained with the static centrifuge technique and the Cavitron are similar to bench dehydration in a short-vesseled species, i.e., a species with no through vessels (open at both ends) in the segment and with few vessels open from the cut surface to the middle of the segment. All centrifuge generated VCs for *H. dactyloides* were sigmoidal and similar to bench dehydration VCs, with a slight shift towards more vulnerable values when using the 14 cm rotor (Figure 2; see Table S2 available as Supplementary Data at *Tree Physiology* Online) as

recently found by Pengxian et al. (2018) in *Acer mono* when comparing in the static centrifuge the 14 cm and 27 cm rotors. Vulnerability curves of other short vesseled angiosperms such as *Betula pendula* (Cochard et al. 2010), *Fagus sylvatica* (Aranda et al. 2014), *Populus tremuloides* (Schreiber et al. 2011) or *Acer negundo* (Christman et al. 2009) were also sigmoidal when the static centrifuge or the Cavitron were used. In contrast, the VC shape obtained for *H. leucoptera* samples differed significantly depending on methodology resulting in a shift of P_{50} of 2 MPa in samples from the same population (Figure 2; see Table S2 available as Supplementary Data at *Tree Physiology* Online). This dramatic change was observed previously in peach (*Prunus persica*) when the length of the centrifuged samples was varied in a Cavitron; shorter samples were more vulnerable to embolism (P_{50} shifted from -4.5 to -1 MPa) and VCs became r-shaped (Cochard et al. 2010). However, when using the static centrifuge to measure the same population, Sperry et al. (Sperry et al. 2012) found that VCs were linear and relatively insensitive to the number of open vessels with P_{50} less negative than -2 MPa using 14 cm and 27 cm samples. This difference in sensitivity to the proportion of open vessels in

the centrifuged samples has led some to conclude that the original centrifuge method and rotor design are not subject to the open vessel artefact (Sperry et al. 2012, Hacke et al. 2015). However, Torres-Ruiz et al. (2017) demonstrated that if the amount of open vessels is relatively high in both rotors, 14 and 27 cm, VCs could be equally biased and would appear statistically indistinguishable.

Recent publications have addressed this controversy, showing that long-vesseled species such as grape vine, oaks, *Robinia* or olive, with a high proportion of open vessels, produce similarly biased results with both the static centrifuge and the Cavitron when compared with reference curves generated by dehydration or non-invasive imaging (Choat et al. 2010, 2016, Torres-Ruiz et al. 2014), Pengxian et al. 2018, Li et al. (2008) and Pengxian et al. (2018) tested the two centrifuge methods head to head and found close correspondence in VCs across species with different xylem anatomy. An extended literature survey of methods to measure vulnerability to embolism showed that when using the centrifuge, VCs were sigmoidal in conifers and in long-vesseled species exponential, whereas in diffuse porous species VCs varied from sigmoidal to linear or exponential (Cochard et al. 2013). Our measurements and simulations made with the CAVITOPEN model explain the different shapes of VCs and some disagreements between the static centrifuge and the Cavitron. In short-vesseled angiosperms, we have shown that VCs by centrifugation agreed with each other and closely matched the curves based on bench dehydration and microCT (Cochard et al. 2010, Choat et al. 2016). In angiosperms with a proportion of vessels open to the middle but not the whole way through, the standard protocol in the static centrifuge produces linear VCs (Sperry et al. 2012). Here the initial conductivity is measured before spinning, thus if the native embolism is low, all the vessels are conductive, regardless of their length. As soon as the sample is spun, the conductivity would be artificially reduced relative to the native state in proportion to the amount of vessels open to centre. Samples with open vessels thus become artificially vulnerable to embolism at the beginning of the VC (i.e., at less negative water potentials). For *H. leucoptera*, this translated into less negative values of P_{12} in all centrifuged samples compared with those measured with the bench dehydration technique creating a linear response or a plateau at high water potentials. Higher differences in P_{12} were observed in *H. leucoptera* than in *H. dactyloides* in accordance with a higher proportion of vessels open to centre in the former species (Figure 1). In the Cavitron, the initial measurement was made while spinning at low tension and many open to centre vessels would already be embolized in the initial measurement of conductivity, resulting in a lower artefactual loss of conductivity in the subsequent water potentials of the VC. This may bias the curves slightly, pushing them to more negative values but it did not appear to be significant effect here as the Cavitron curves for *H. leucoptera* were similar to bench dehydration curves.

The simulations of PLC with the CAVITOPEN model confirmed that the impact of open vessels on the VC was higher when vessels were long, samples short and when open vessels cavitated at less negative pressures (Figure 4). If the samples were much shorter than the maximum vessel length of the branch (see the results in Figure 4 for the 14 cm rotor with L_{max} 50 cm), the resulting VC was exponential (r-shaped), as observed in long-vesseled angiosperms, and shifted to more linear or s-shaped when L_{max} was decreased or the sample length increased. One of the assumptions in the model is that vessels open at the cut surface cavitate when they reach a threshold value that is far less negative than intact vessels whose two ends are included within the spun segment. This influences the shape the VC at higher pressures creating a 'bump' in the VC followed by a plateau. This effect can be corrected to some extent if the first inflexion point of the VC is considered to be the 0% point for loss of conductivity. In this case the initial conductivity (K_i) value is shifted to a lower value corresponding to the hydraulic conductivity of the plateau (Figure 4D). The estimated values of P_{50} and S_{50} when the CAVITOPEN model was fit to actual measurements agreed quite well with those obtained with reference techniques and confirmed that this model can be used to correct open vessel artefacts for centrifuge-based VCs. The estimated L_{max} was, however, significantly shorter than L_{max} measured with the air injection technique. The air injection technique has shown to produce higher L_{max} than the rubber injection method (Pan et al. 2015); thus our values could be overestimated. On the other hand, the model assumed that vessel lengths in a sample follow the density function proposed by Cohen et al. (2003), which can be sensitive to the clustering of vessel lengths (Cai and Tyree 2014). It is clear that the actual distribution of vessel lengths, network topology and connectivity are crucial for the sensitivity to an open vessel artefact.

Origin of the open-vessel artefact

The physical mechanisms underlying this open-vessel artefact are yet to be fully elucidated. Some studies suggest that microbubbles and particles can act as nucleation sites when they flow through the sample as it spins in the Cavitron, causing premature embolism (Cochard et al. 2010, Sperry et al. 2012, Wang et al. 2014). In the static centrifuge, bubbles might be drawn into vessels while starting the spin or while mounting or dismounting the stems to measure flow (Wang et al. 2014). In both centrifuge techniques bubbles in open vessels can move by buoyancy while spinning toward the region of lowest pressure at the centre of rotation (Rockwell et al. 2014). Draining from open vessels as a consequence of artefactual embolism when the centrifuge starts spinning appears to be a common phenomenon in both rotors. Our microCT images showed that after spinning in the centrifuge, most of the vessels were empty near the ends even though tension ought to be zero (Cochard et al. 2005). The use of water saturated foam pads to avoid desiccation did not prevent this

(Tobin et al. 2013, Hacke et al. 2015). We discarded the possibility that sample manipulation before spinning or during wax embedding had triggered vessel draining because we scanned control samples that were not spun. These samples showed no embolism (Figure 3). Furthermore, patterns of embolism did not follow theoretical expectations based on the distribution of tension within the spun sample. The embolism levels decreased from the ends to the centre in a fashion consistent with the amount of vessels open to centre, opposite to that expected from profile in tension and in agreement with the assumption of the CAVITOPEN model than open vessels artificially cavitate when they reach a threshold pressure that is much less negative than in intact vessels. This pattern was observed at water potentials inducing less than 40% loss of conductivity based on the VC obtained using the middle segment of the centrifuged sample (Figure 3), even though the centre of the sample experienced the highest tensions. Embolism levels converged within the sample at -9 MPa at 80–90%. These results confirm that centrifugation drains open vessels and only reliably measure the vulnerability of intact xylem vessels within the sample (see Figure S1 available as Supplementary Data at *Tree Physiology* Online). This is consistent with observations made previously by Cochard et al. (2010) using the Cavitrone; they reported that embolism was higher in the basal and upstream ends relative to the centre of samples from species with vessels that are predominately at least half as long as the spun segment. Cai et al. (2010) and Pengxian et al. (2018) also reported higher PLC values than predicted by theory at both ends after spinning samples in a Cavitrone. Given that our results were obtained with the static centrifuge it is clear that the overestimation of vulnerability for open to centre vessels occurs in both versions of the centrifuge technique.

The hydraulic continuity between vessels cut open at each end of the sample and vessels with their terminal ends in this portion of the sample is probably re-established by refilling of vessels immersed under water at both ends (Figure 2 in Cochard et al. (2010)). This refilling would occur by capillarity either while spinning in the Cavitrone or while flow is measured gravimetrically (see Figure S2 available as Supplementary Data at *Tree Physiology* Online). Since the middle of the centrifuged sample contains the majority of intact vessels, VCs constructed with the static centrifuge technique of angiosperm species using only the central segment are more reliable and in closer agreement with PLC generated by natural dehydration (Figure 2). This modification is technically easy to achieve and mitigates the open vessel artefact; however, it carries the disadvantage that samples cannot be spun repeatedly to construct replicate curves for each sample and thus more plant material is needed to construct each curve.

Conclusion

We confirmed the validity of VCs constructed with both centrifuge methods for short conduit angiosperm species, those with

most conduits shorter than half the length of the centrifuge rotor. A new model, CAVITOPEN, was developed to simulate the effect of vessel length, rotor size and vulnerability of open vessels in loss of conductivity of centrifuged samples. In species with maximum vessel length similar to the centrifuge rotor, we recommend constructing VCs with the Cavitrone or measuring flow exclusively in the central part of the spun segment when using the static centrifuge. Alternatively, artefactual embolism at low xylem tensions can be corrected if the first inflexion point of the VC is considered to be the starting point for K_{\max} (0% loss of conductivity) or by fitting the CAVITOPEN model to the measurements to estimate P_{50} and S_{50} . When samples contain a high proportion of open to centre vessels, the centrifuge technique is prone to error and overestimates vulnerability to embolism. Determining the proportion of open to centre vessels or performing the simple test recently proposed by Torres-Ruiz et al. (2017), which compares changes in K_s before and after spinning in the centrifuge at low tensions, are highly advisable before using any of the centrifuge techniques.

The shape of the VCs obtained with bench dehydration was always sigmoidal while in centrifuged samples the shape was determined by the presence of open vessels. While previous studies have demonstrated that species with the longest vessel classes (e.g., lianas, ring porous trees) open vessels tend to exhibit exponential curves when measured in the centrifuge. Here we showed that VCs with a linear shape are symptomatic of species with intermediate vessel lengths in which a higher proportion of vessels open to centre of the test segment. The occurrence of this incipient open vessel artefact can be mitigated by measurement of the excised central portion of the segment.

Supplementary Data

Supplementary Data for this article are available at *Tree Physiology* Online.

Acknowledgments

We thank Dr Javier Cano, Adrián Cano, Teresa Rosas and Jennifer Peters for field assistance, Dr Iain M. Young for X-ray microCT advice and comments on the manuscript, Gavin McKenzie for lab support and Dr Stephanie Stuart for her ideas and writing assistance. No conflict of interests declared.

Conflict of interest

None declared.

Funding

Rosana López was supported by a Marie Curie Fellowship from the European Union Seventh Framework Programme (FP7/2007-2013) under grant agreement n° [IOF-624473]. Brendan Choat was

supported by an Australian Research Council Future Fellowship (FT130101115).

References

- Alder N, Pockman W, Sperry J, Nuismer S (1997) Use of centrifugal force in the study of xylem cavitation. *J Exp Bot* 48:665–674.
- Aranda I, Cano FJ, Gascó A, Cochard H, Nardini A, Mancha JA, López R, Sánchez-Gómez D (2014) Variation in photosynthetic performance and hydraulic architecture across European beech (*Fagus sylvatica* L.) populations supports the case for local adaptation to water stress. *Tree Physiol* 35:34–46.
- Brodersen CR, McElrone AJ, Choat B, Lee EF, Shackel KA, Matthews MA (2013) In vivo visualizations of drought-induced embolism spread in *Vitis vinifera*. *Plant Physiol* 161:1820–1829.
- Brodribb TJ (2017) Progressing from 'functional' to mechanistic traits. *New Phytol* 215:9–11.
- Brodribb TJ, Cochard H (2009) Hydraulic failure defines the recovery and point of death in water-stressed conifers. *Plant Physiol* 149:575–584.
- Cai J, Tyree MT (2014) Measuring vessel length in vascular plants: can we divine the truth? History, theory, methods, and contrasting models. *Trees* 28:643–655.
- Cai J, Hacke U, Zhang S, Tyree MT (2010) What happens when stems are embolized in a centrifuge? Testing the cavitron theory. *Physiol Plant* 140:311–320.
- Choat B, Drayton WM, Brodersen C, Matthews MA, Shackel KA, Wada H, McElrone AJ (2010) Measurement of vulnerability to water stress-induced cavitation in grapevine: a comparison of four techniques applied to a long-vessel species. *Plant Cell Environ* 33:1502–1512.
- Choat B, Jansen S, Brodribb TJ et al (2012) Global convergence in the vulnerability of forests to drought. *Nature* 491:752–755.
- Choat B, Badel E, Burrett R, Delzon S, Cochard H, Jansen S (2016) Noninvasive measurement of vulnerability to drought-induced embolism by X-ray microtomography. *Plant Physiol* 170:273–282.
- Choat B, Brodribb TJ, Brodersen CR, Duursma RA, López R, Medlyn BE (2018) Triggers of tree mortality under drought. *Nature* 558:531–539.
- Christman MA, Sperry JS, Adler FR (2009) Testing the 'rare pit' hypothesis for xylem cavitation resistance in three species of *Acer*. *New Phytol* 182:664–674.
- Cobb AR, Choat B, Holbrook NM (2007) Dynamics of freeze-thaw embolism in *Smilax rotundifolia* (Smilacaceae). *Am J Bot* 94:640–649.
- Cochard H (2002) A technique for measuring xylem hydraulic conductance under high negative pressures. *Plant Cell Environ* 25:815–819.
- Cochard H, Ewers F, Tyree M (1994) Water relations of a tropical vine-like bamboo (*Rhipidocladum racemiflorum*): root pressures, vulnerability to cavitation and seasonal changes in embolism. *J Exp Bot* 45:1085–1089.
- Cochard H, Damour G, Bodet C, Tharwat I, Poirier M, Améglio T (2005) Evaluation of a new centrifuge technique for rapid generation of xylem vulnerability curves. *Physiol Plant* 124:410–418.
- Cochard H, Herbette S, Barigah T, Badel E, Ennajeh M, Vilagrosa A (2010) Does sample length influence the shape of xylem embolism vulnerability curves? A test with the Cavitron spinning technique. *Plant Cell Environ* 33:1543–1552.
- Cochard H, Badel E, Herbette S, Delzon S, Choat B, Jansen S (2013) Methods for measuring plant vulnerability to cavitation: a critical review. *J Exp Bot* 64:4779–4791.
- Cochard H, Delzon S, Badel E (2015) X-ray microtomography (micro-CT): a reference technology for high-resolution quantification of xylem embolism in trees. *Plant Cell Environ* 38:201–206.
- Cohen S, Bennink J, Tyree M (2003) Air method measurements of apple vessel length distributions with improved apparatus and theory. *J Exp Bot* 54:1889–1897.
- Dalla-Salda G, Fernández ME, Sergent A-S, Rozenberg P, Badel E, Martínez-Meier A (2014) Dynamics of cavitation in a Douglas-fir tree-ring: transition-wood, the lord of the ring? *J Plant Hydraulics* 1:005.
- Duursma R (2017) An R implementation of the CAVITOPEN model (R package). [WWW document]. <https://github.com/RemkoDuursma/cavitopen>.
- Duursma R, Choat B (2017) fitplc-an R package to fit hydraulic vulnerability curves. *J Plant Hydraul* 4:002.
- Ennajeh M, Simoes F, Khemira H, Cochard H (2011) How reliable is the double-ended pressure sleeve technique for assessing xylem vulnerability to cavitation in woody angiosperms? *Physiol Plant* 142:205–210.
- Ewers FW, Fisher JB (1989) Variation in vessel length and diameter in stems of six tropical and subtropical lianas. *Am J Bot* 76:1452–1459.
- Hacke UG, Venturas MD, MacKinnon ED, Jacobsen AL, Sperry JS, Pratt RB (2015) The standard centrifuge method accurately measures vulnerability curves of long-vessel olive stems. *New Phytol* 205:116–127.
- Holbrook NM, Burns MJ, Field CB (1995) Negative xylem pressures in plants: a test of the balancing pressure technique. *Science* 270:1193–1195.
- Jacobsen AL, Pratt RB (2012) No evidence for an open vessel effect in centrifuge-based vulnerability curves of a long-vessel liana (*Vitis vinifera*). *New Phytol* 194:982–990.
- Jansen S, Schuldt B, Choat B (2015) Current controversies and challenges in applying plant hydraulic techniques. *New Phytol* 205:961–964.
- Li Y, Sperry JS, Taneda H, Bush SE, Hacke UG (2008) Evaluation of centrifugal methods for measuring xylem cavitation in conifers, diffuse- and ring-porous angiosperms. *New Phytol* 177:558–568.
- Nardini A, Battistuzzo M, Savi T (2013) Shoot desiccation and hydraulic failure in temperate woody angiosperms during an extreme summer drought. *New Phytol* 200:322–329.
- Nolf M, Lopez R, Peters JM, Flavel RJ, Koloadin LS, Young IM, Choat B (2017) Visualization of xylem embolism by X-ray microtomography: a direct test against hydraulic measurements. *New Phytol* 214:890–898.
- Ogle K, Barber JJ, Willson C, Thompson B (2009) Hierarchical statistical modeling of xylem vulnerability to cavitation. *New Phytol* 182:541–554.
- Pan R, Geng J, Cai J, Tyree MT (2015) A comparison of two methods for measuring vessel length in woody plants. *Plant Cell Environ* 38:2519–2526.
- Pengxian Y, Feng M, Qing L, Rui A, Jing C, Guangyuan D (2018) A comparison of two centrifuge techniques for constructing vulnerability curves: insight into the 'open-vessel' artifact. *Physiol Plant*. doi: 10.1111/ppl.12738
- Pockman WT, Sperry JS, Leary JW (1995) Sustained and significant negative water pressure in xylem. *Nature* 378:715.
- Rockwell FE, Wheeler JK, Holbrook NM (2014) Cavitation and its discontents: opportunities for resolving current controversies. *Plant Physiol* 164:1649–1660.
- R Core Team. 2015. R: a language and environment for statistical computing. Vienna, Austria: R Foundation for Statistical Computing. [WWW document]. <http://www.R-project.org/>
- Rodríguez-Calcerrada J, Li M, López R, Cano FJ, Oleksyn J, Atkin OK, Pita P, Aranda I, Gil L (2017) Drought-induced shoot dieback starts with massive root xylem embolism and variable depletion of nonstructural carbohydrates in seedlings of two tree species. *New Phytol* 213:597–610.
- Sala A, Piper F, Hoch G (2010) Physiological mechanisms of drought-induced tree mortality are far from being resolved. *New Phytol* 186:274–281.

- Schneider CA, Rasband WS, Eliceiri KW (2012) NIH Image to ImageJ: 25 years of image analysis. *Nat Methods* 9:671–675.
- Schreiber SG, Hacke UG, Hamann A, Thomas BR (2011) Genetic variation of hydraulic and wood anatomical traits in hybrid poplar and trembling aspen. *New Phytol* 190:150–160.
- Sperry JS (1985) Xylem embolism in the palm *Rhapis excelsa*. *IAWA J* 6: 283–292.
- Sperry JS, Tyree MT (1988) Mechanism of water stress-induced xylem embolism. *Plant Physiol* 88:581–587.
- Sperry JS, Christman MA, Torres-Ruiz JM, Taneda H, Smith DD (2012) Vulnerability curves by centrifugation: is there an open vessel artefact, and are 'r' shaped curves necessarily invalid? *Plant Cell Environ* 35:601–610.
- Tobin MF, Pratt RB, Jacobsen AL, De Guzman ME (2013) Xylem vulnerability to cavitation can be accurately characterised in species with long vessels using a centrifuge method. *Plant Biol* 15:496–504.
- Torres-Ruiz JM, Cochard H, Mayr S, Beikircher B, Diaz-Espejo A, Rodriguez-Dominguez CM, Badel E, Fernandez JE (2014) Vulnerability to cavitation in *Olea europaea* current-year shoots: further evidence of an open-vessel artifact associated with centrifuge and air-injection techniques. *Physiol Plant* 152:465–474.
- Torres-Ruiz JM, Jansen S, Choat B et al (2015) Direct X-ray microtomography observation confirms the induction of embolism upon xylem cutting under tension. *Plant Physiol* 167:40–43.
- Torres-Ruiz JM, Cochard H, Mencuccini M, Delzon S, Badel E (2016) Direct observation and modelling of embolism spread between xylem conduits: a case study in Scots pine. *Plant Cell Environ* 39:2774–2785.
- Torres-Ruiz JM, Cochard H, Choat B et al (2017) Xylem resistance to embolism: presenting a simple diagnostic test for the open vessel artefact. *New Phytol* 215:489–499.
- Tyree MT, Dixon MA (1986) Water stress induced cavitation and embolism in some woody plants. *Physiol Plant* 66:397–405.
- Tyree MT, Sperry JS (1988) Do woody plants operate near the point of catastrophic xylem dysfunction caused by dynamic water stress? answers from a model. *Plant Physiol* 88:574–580.
- Tyree MT, Zimmermann MH (2002) Hydraulic architecture of whole plants and plant performance Xylem structure and the ascent of sap. Springer, Berlin, Heidelberg, pp 175–214.
- Urlı M, Porte AJ, Cochard H, Guengant Y, Burlett R, Delzon S (2013) Xylem embolism threshold for catastrophic hydraulic failure in angiosperm trees. *Tree Physiol* 33:672–683.
- Venturas MD, MacKinnon ED, Dario HL, Jacobsen AL, Pratt RB, Davis SD (2016) Chaparral shrub hydraulic traits, size, and life history types relate to species mortality during California's historic drought of 2014. *PLoS One* 11:e0159145.
- Wang R, Zhang L, Zhang S, Cai J, Tyree MT (2014) Water relations of *Robinia pseudoacacia* L.: do vessels cavitate and refill diurnally or are R-shaped curves invalid in Robinia? *Plant Cell Environ* 37: 2667–2678.
- Wheeler JK, Huggett BA, Tofte AN, Rockwell FE, Holbrook NM (2013) Cutting xylem under tension or supersaturated with gas can generate PLC and the appearance of rapid recovery from embolism. *Plant Cell Environ* 36:1938–1949.